

# An Analogous Periodic Law for Strong Anchoring of Polysulfides on Polar Hosts in Lithium Sulfur Batteries: S- or Li-Binding on First-Row Transition-Metal Sulfides?

Xiang Chen,<sup>†,⊥</sup> Hong-Jie Peng,<sup>†,⊥</sup> Rui Zhang,<sup>†</sup> Ting-Zheng Hou,<sup>†,‡</sup> Jia-Qi Huang,<sup>†,§</sup> Bo Li,<sup>||</sup> and Qiang Zhang<sup>\*,†,||</sup>

<sup>†</sup>Beijing Key Laboratory of Green Chemical Reaction Engineering and Technology, Department of Chemical Engineering, Tsinghua University, Beijing 100084, China

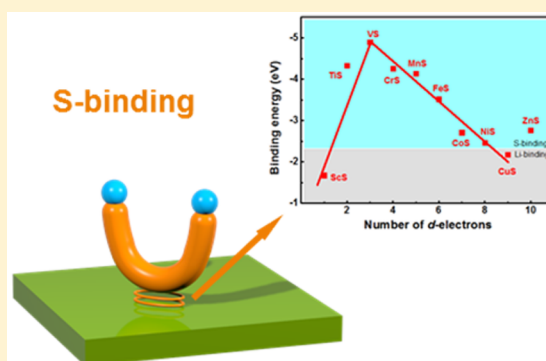
<sup>‡</sup>Department of Materials Science and Engineering, University of California Berkeley, Berkeley, California 94720, United States

<sup>§</sup>Advanced Research Institute for Multidisciplinary Science, Beijing Institute of Technology, Beijing 100081, China

<sup>||</sup>Shenyang National Laboratory for Materials Science, Institute of Metal Research, Chinese Academy of Sciences, 72 Wenhua Road, Shenyang 110016, China

## Supporting Information

**ABSTRACT:** Lithium–sulfur (Li–S) batteries are strongly considered for next-generation energy storage devices. However, severe issues such as the shuttle of polysulfides restrict their practical applications. Exploring the design principle of anchoring polysulfides physically and chemically through the polar substrate is therefore highly necessary. In this Letter, first-row transition-metal sulfides (TMSs) are selected as the model system to obtain a general principle for the rational design of a sulfur cathode. The strong S-binding that is induced by charge transfer between transition-metal atoms in TMS slabs and S atoms in Li<sub>2</sub>S is confirmed to be of great significance in TMS composite cathodes. An analogous periodic law is proposed, which is also extended to first-row TM oxides. VS has the strongest anchoring effects on Li<sub>2</sub>S immobilization and a relatively low lithium ion diffusion barrier. The binding energies and Li diffusion properties are considered as the key descriptors for the rational design of sulfur cathodes.



The robust and facile use of sustainable energy sources is one of the most critical elements of modern society to meet growing energy demands. Energy storage devices with high energy densities are therefore essential. Lithium–sulfur (Li–S) batteries are strongly considered as one of the potential candidates for next-generation energy storage because of their extremely high energy density (2600 Wh kg<sup>−1</sup>) and are attracting growing interests.<sup>1</sup> Furthermore, sulfur possesses the advantages of being an abundant resource and having a low cost and high biocompatibility, which are particularly attractive for bulk applications toward reliable energy storage.<sup>2–10</sup> However, there are significant issues raised by the low electrical conductivity, volume change of the sulfur cathode during cycling, and the well-known “shuttle” of soluble polysulfides. These issues result in the low utilization of sulfur, poor cycling life, low efficiency, and severe self-discharge, all of which prevent the practical application of Li–S batteries.<sup>11–19</sup>

Over the past years, tremendous efforts have been devoted to these challenging issues. In particular, the incorporation of sulfur into conductive porous materials (such as porous carbon,<sup>20</sup> carbon spheres,<sup>21</sup> carbon nanotubes,<sup>22</sup> graphene,<sup>23–27</sup> graphene oxides,<sup>28,29</sup> and their hybrids<sup>30–33</sup>) can well ameliorate the issues of low electrical conductivity and volume change to a large extent. However, there is still a lack of efficient strategies solving the polysulfide shuttle because of the weak binding between routine nonpolar carbon materials and polar polysulfides.

For an enhanced anchoring strength of polar polysulfides on carbon, heteroatom doping has been adopted.<sup>34,35</sup> Owing to the favorable guest–host interactions to bind polar sulfur

Received: February 26, 2017

Accepted: March 9, 2017

Published: March 9, 2017

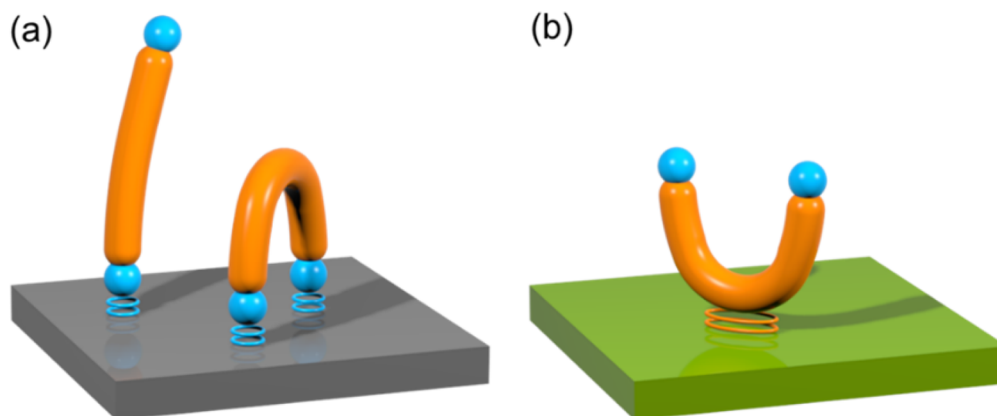


**Figure 1.** Schematic diagrams of polysulfides anchored on the polar host surface through (a) Li-binding in heteroatom-doped nanocarbon cathodes and (b) S-binding in metal sulfide cathodes.

species, nitrogen-doped carbon emerged as an efficient host to render Li–S batteries with improved reversibility and stability.<sup>36</sup> Reactive oxygen-functional groups attached to carbon materials such as graphene oxide were also effective for polysulfide immobilization.<sup>28</sup> Particularly, Hou et al. systematically investigated different heteroatom dopants using density functional theory (DFT) methods and proposed a general design principle for doped nanocarbon materials.<sup>37</sup> A volcano plot in regards to binding energies to polysulfides was presented with N- and O-doping on the top. It was also predicted that N and O codoped graphene facilitated a stronger anchoring interaction, which was verified by recent reports.<sup>38</sup> In addition, N and B codoped carbon materials show enhanced performance when used as a sulfur cathode, further demonstrating the codoping effects resulting in stronger dipoles.<sup>39,40</sup>

Apart from heteroatom doping, various metal oxides, sulfides, nitrides, and carbides have been used as noncarbonaceous polar hosts in sulfur cathodes.<sup>15,41–49</sup> On one hand, a part of these components exhibited strong interactions with polysulfides to suppress the shuttle effect. On the other hand, several polar hosts that have been a part of these components are proven to promote the transformation between polysulfides. Tao et al. suggested that a balance between the adsorption and diffusion of polar sulfur species should be considered as a design principle of sulfur hosts, which was revealed by a systematic comparison between various nonconductive metal oxides.<sup>50</sup>

Unlike metal oxides sulfur hosts, their sulfide counterparts, especially transition metal (TM) sulfides (TMSs), usually exhibit higher electrical conductivities owing to the more covalent nature endowed by soft basic  $S^{2-}/S_2^{2-}$  ions instead of the hard basic  $O^{2-}$  ion. Moreover, the soft acid–soft base interactions between TM cations and  $S^{2-}/S_2^{2-}$  anions render TM atoms with a higher density of valence electrons in sulfides than in oxides, which enables TM as binding sites for extrinsic adsorbates such as polysulfides. Therefore, TMSs hold great promise as advanced sulfur hosts. For example, Nazar and co-workers<sup>51</sup> reported a metallic  $Co_9S_8$  material with an interconnected graphene-like nanoarchitecture for sulfur cathode, achieving better cycling stability (fade <0.045% per cycle over 1500 cycles at C/2) and a high sulfur loading (75 wt % sulfur and 4.5 mg  $cm^{-2}$  areal sulfur loading) at the same time; sulfiphilic  $CoS_2$  incorporated carbon/sulfur cathodes exhibited promoted energy efficiency (increased by 10% compared with normal carbon/sulfur cathodes), promised high discharge

capacity (a high initial capacity of 1368 mAh  $g^{-1}$  at 0.5 C), and stable cycling performance for 2000 cycles (a slow capacity decay rate of 0.034%/cycle at 2.0 C).<sup>52</sup> Very recently, Cui and co-workers<sup>42</sup> investigated a series of TMSs as a platform to probe processes of  $Li_2S$  oxidation and polysulfide adsorption. It was found that energy barriers for  $Li_2S$  decomposition on various TMS surfaces were associated with the bindings between lithium cations and sulfur anions in TMSs and impacted significantly on the overpotential of  $Li_2S$  oxidation. It is highly expected to gain atomic insights into the detailed interactions between polysulfides and polar substrates through theoretical tools such as density functional theory (DFT). Exploring the intrinsic differences between a series of analogous host materials such as TMSs is a necessary step to draw general design principles from broader material families either studied or under investigation.

In this contribution, we selected first-row TMSs as platforms and investigated their intrinsic differences systematically. DFT, as a powerful theoretical tool, was employed to obtain both the binding energy to  $Li_2S$  and lithium diffusion barrier on various TMS surfaces. The theoretical calculation drew an atomic scheme including the following: (1) S-binding was preferable to Li-binding. (2) VS exhibited the highest binding energy of  $-4.89$  eV. (3) Small lithium diffusion barriers less than 0.30 eV were obtained on most of first-row TMS surfaces. This work deepens understanding of TMSs as polar sulfur hosts. General principles were proposed for rational screening and design of scaffolding materials to achieve superb performance of Li–S batteries.

For existing host materials such as heteroatom-doped carbon and TMSs, two atomic binding configurations are usually obtained from a theoretical perspective. One is based on the “lithium bond” theory.<sup>37</sup> For most of the doped carbon hosts, polysulfides are bonded through dipole–dipole interactions of Li–X (X represents the heteroatoms such as O, N, etc.) (Figure 1a). For TMSs, polysulfides are adsorbed through the TM–S bond, where the sulfur is from extrinsic adsorbates such as  $Li_2S$  and polysulfides. Such a TM–S bond plays an important role (Figure 1b). In previous reports, the two binding configurations, namely Li-binding and S-binding, were found to coexist to afford strong anchoring as well as excellent lithium diffusion properties.<sup>42,53</sup> However, the main difference between these two binding configurations remains concealed. Moreover, the intrinsic differences between diverse TMSs and how these differences determine the atomic behaviors have not been fully

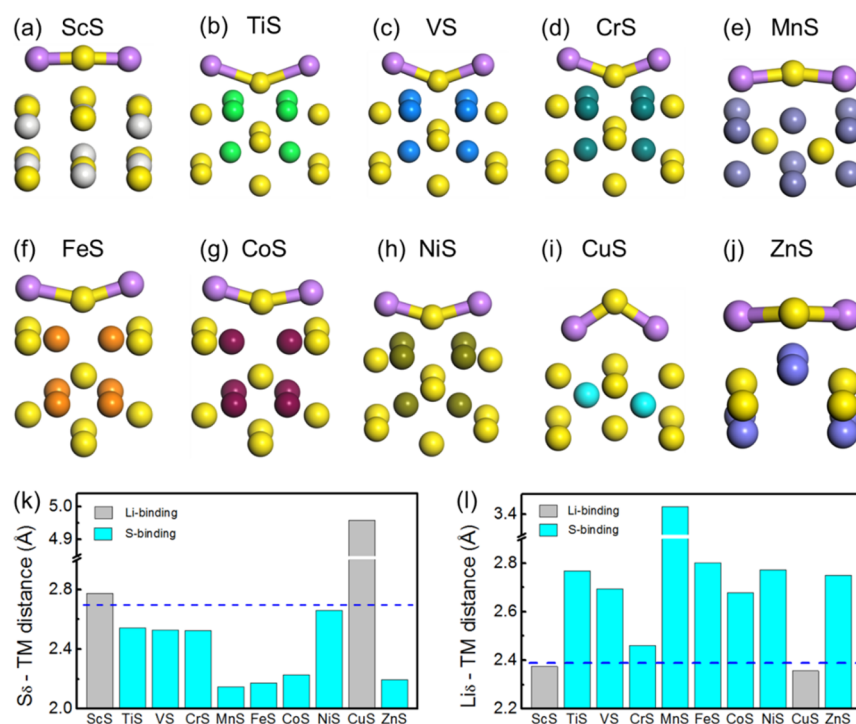


Figure 2. Optimized structures of (a) ScS, (b) TiS, (c) VS, (d) CrS, (e) MnS, (f) FeS, (g) CoS, (h) NiS, (i) CuS, and (j) ZnS (001) surfaced bound with  $\text{Li}_2\text{S}$  molecule. (k)  $\text{S}_\delta$ -TM distance and (l)  $\text{Li}_\delta$ -TM distance in the above-optimized structure. The lithium and sulfur atoms in  $\text{Li}_2\text{S}$  are marked with purple and yellow, respectively. S atoms in the slabs are marked with yellow. Metal atoms in the slabs are marked with the corresponding colors shown above.

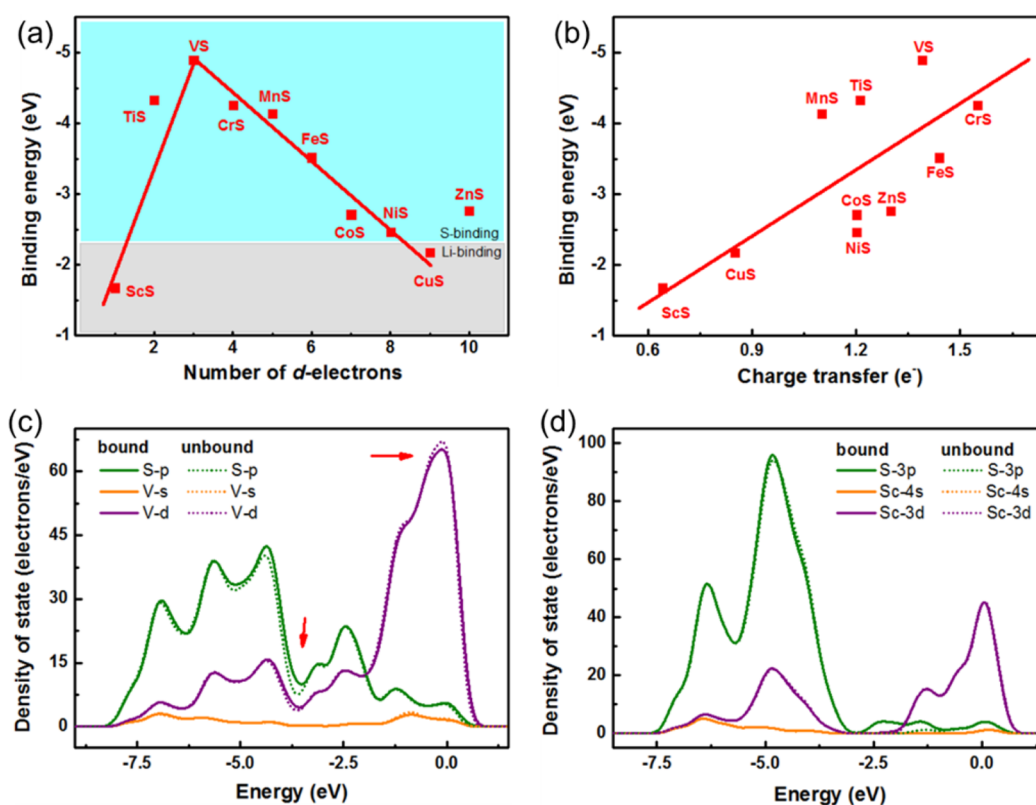


Figure 3. (a) Periodic law of binding energy. (b) Linear relationship of binding energy vs charge transfer. PDOS analysis of (c) VS and (d) ScS. The solid and dotted lines refer to the PDOS of TMSs bound and unbound with  $\text{Li}_2\text{S}$ , respectively.

understood yet. Disclosing these mysteries would be of great importance to provide rational guidance.

First-row TMSs with the most stable and simplest structures, including ScS, TiS, VS, CrS, MnS, FeS, CoS, NiS, CuS, and

ZnS, were considered, and their primary structures were collected from Materials Project Database.<sup>54</sup> As summarized in Table S1, ScS, CuS, ZnS, and MnS have a cubic structure with a space group of *Fm3m* [225] for the former three and *F43m* [216] for MnS. FeS exhibits a tetragonal structure with a space group of *P4/nmm* [129]. The other TMSs possess a hexagonal structure with a space group of *P6<sub>3</sub>/nmc* [194]. All of these TMSs except ZnS have a zero band gap, implying the metallic nature of most of the first-row TMSs (Figure S1). It should be noted that first-row TM disulfides are more common than first-row TMSs in Li–S battery research. For TM monosulfides, only FeS has been studied previously.<sup>42</sup> Nevertheless, in existing studies, TMs generally possessed various valences from +2 to +4, making direct comparisons difficult. In this contribution, however, TMSs have analogous structures and identical valence (+2) of TMs, simplifying the parameter matrices. Based on that, general principles can be derived.

Figures 2 and S2 illustrate the optimized structures of TMSs with a Li<sub>2</sub>S molecule bound. The Mulliken charge and bond length are presented as well. The two binding configurations are demonstrated. ScS and CuS exhibit a Li-binding configuration that Li in Li<sub>2</sub>S (denoted as Li<sub>δ</sub> where δ refers to Li<sub>2</sub>S) binds to S in TMSs to form Li<sub>δ</sub>–S bonds. The other TMSs dominate a S-binding configuration of S<sub>δ</sub>–TM. The former one is analogous to that for heteroatom-doped carbon, which has been extensively investigated.<sup>37</sup> The latter has been indicated in only few very recent reports. The VS is exemplified to reveal the detailed S<sub>δ</sub>–TM bond nature (Figure 2c and S2c). The Li<sub>2</sub>S molecule interacts with VS through S-binding, and the S<sub>δ</sub> is bound at the bridge site. The distance between S<sub>δ</sub> and V attached is calculated to be 0.254 nm (Figure 2k and S2c), quite close to the V–S bond length in VS crystal (0.239 nm, Table S2). That suggests a binding strength between Li<sub>2</sub>S and VS that is as strong as that in bulk VS crystal. Meanwhile, the distance between Li<sub>δ</sub> and S in VS is 0.269 nm, much larger than that in the molecule (0.210 nm) (Figures 2l, S2c, and S3). Moreover, the Mulliken charge of the adsorbed Li<sub>2</sub>S is much different from that of the pristine Li<sub>2</sub>S molecule in vacuum (Figures S2c and S3). Change in the Mulliken charge of Li<sub>δ</sub> is almost negligible, from 0.890 to 0.970 after adsorption. In contrast, the change in the Mulliken charge of S<sub>δ</sub> is significant, from –1.780 to –0.550 after adsorption. That indicates the huge electron transfer from S<sub>δ</sub> to TMSs, or equivalently, the formation of a S<sub>δ</sub>–V chemical bond. The chemical bond formation is believed to be the origin of the strong anchoring effect.

To obtain a universal scheme, the binding energy, which has a strong linear relationship with and is induced by the charge transfer, is plotted with respect to the electron number of the d-orbital (Figure 3a,b and Tables S3 and S4). Similar to the case of VS, electrons are transferred from S<sub>δ</sub> in adsorbed Li<sub>2</sub>S to TMs in TMS slabs, and the transferred electrons mainly occupy the d-orbitals of TMs. Consequently, the binding energy is closely related to the d-orbitals with a periodic law to describe such a relationship. From ScS to VS and from VS to ZnS, respectively, there are two nearly linear scaling lines. VS lies on the top. Such a unique periodic law is ascribed to the counterbalance between the valence electron number and the unoccupied d-orbital number. For early TMSs such as ScS and TiS, the divalent TM cations, Sc<sup>2+</sup> and Ti<sup>2+</sup>, have insufficient valence electrons (1 for Sc<sup>2+</sup> and 2 for Ti<sup>2+</sup>). Therefore, the deficiency in valence electrons prevents the formation of extra chemical bonds of S<sub>δ</sub>–Sc and S<sub>δ</sub>–Ti. For TMSs with a valence electron number larger than 4 in corresponding divalent TM

cations (from Cr<sup>2+</sup> to Cu<sup>2+</sup>), their binding energy to Li<sub>2</sub>S decreases as the valence electron number increases. That is in good accordance with the decrease of unoccupied d-orbital number as well. The decrease in unoccupied d-orbital number also results in difficulty in bond formation of S<sub>δ</sub>–TM. For example, Cu<sup>2+</sup> has nine valence electrons and thereby only one d-orbital with a vacancy to interact with the valence electrons of S<sub>δ</sub>. The deviation of ZnS results from the fully occupied 3d orbitals so that transferred electrons will occupy the 4s orbital. Therefore, the binding energy is not associated with the other TMSs. Besides, Li<sub>2</sub>S lies on ZnS (100) surface, much different from the other binding structures. Similar exceptions to d-band model<sup>55,56</sup> have been reported in chemisorption on metal surfaces, mainly associated with the adsorbates having almost completely filled valence shell, and the substrates with nearly fully occupied d-band, e.g., OH, F, or Cl adsorption on metals and alloys characterized by d<sup>9</sup> or d<sup>10</sup> substrate surface atoms.<sup>57</sup> The reason why VS is on the top is possibly because of the three valence electrons of V<sup>2+</sup>. As a result, valence electrons from S<sub>δ</sub> can appropriately pair the three single electrons of V<sup>2+</sup> to stabilize the binding configurations of Li<sub>2</sub>S on VS. The strong anchoring effect of VS was verified by the visualized adsorption experiments and post-mortem analysis of the electrodes after cycling in recent reports, in which VS<sub>2</sub> showed the best adsorption functions among the selected first-row TM disulfides.<sup>42</sup> Therefore, VS is expected to render the strongest interaction with the Li<sub>2</sub>S molecule.

First-row TM oxides (TMOs) are also considered to extend the periodic law discussed above (Figure S4). A similar volcano-like relationship was found for the TMO system to bind Li<sub>2</sub>S. The only difference, that there is no clear boundary between S-binding and Li-binding, originates from the stronger electronegativity of oxygen than that of sulfur. Such a stronger electronegativity results in a Li<sub>δ</sub>–O bond that is stronger than the Li<sub>δ</sub>–S bond. As a result, in TMOs Li-binding is more predominant than in TMSs. Hopefully, similar periodic laws are expected for transition-metal nitride and metal carbide systems to interact with Li<sub>2</sub>S, demanding further investigation. The periodic law of the binding energy in metallic compounds provides simple but efficient guidance for screening host materials, targeting strong anchoring and suppression of the shuttle effect.

To further understand the S-binding between Li<sub>2</sub>S and TMSs, projected density of states (PDOS) analysis is presented (Figures 3c,d and S5). Concretely, there are obvious changes in PDOS of VS before and after binding Li<sub>2</sub>S, indicating the obvious electron transfer. The changes in 3d-orbitals of V and 3p-orbitals of S indicate the possible d–p orbital interaction, namely, S<sub>δ</sub>–V bond formation, and that the S-binding dominates. In contrast, there is almost no change in PDOS of 3d-orbitals of Sc, implying that the S<sub>δ</sub>–Sc bond is not formed in Li-binding configuration. In Figure S5, PDOS of other TMSs are presented, indicating the distinctive two binding configurations as suggested in Figure 3a. Generally, a TMS possessing S-binding configuration is featured by changes in 3d-orbitals of TM.

As demonstrated above, most of the first-row TMSs, especially VS, can anchor polysulfides efficiently through S-binding, suppressing the shuttle effect and achieving better battery performance. Furthermore, the surface diffusion properties of TMSs are probed as the surface diffusion impacts significantly on the growth of Li<sub>2</sub>S. An uncontrolled deposition results in a low utilization of active substrates and poor cycling



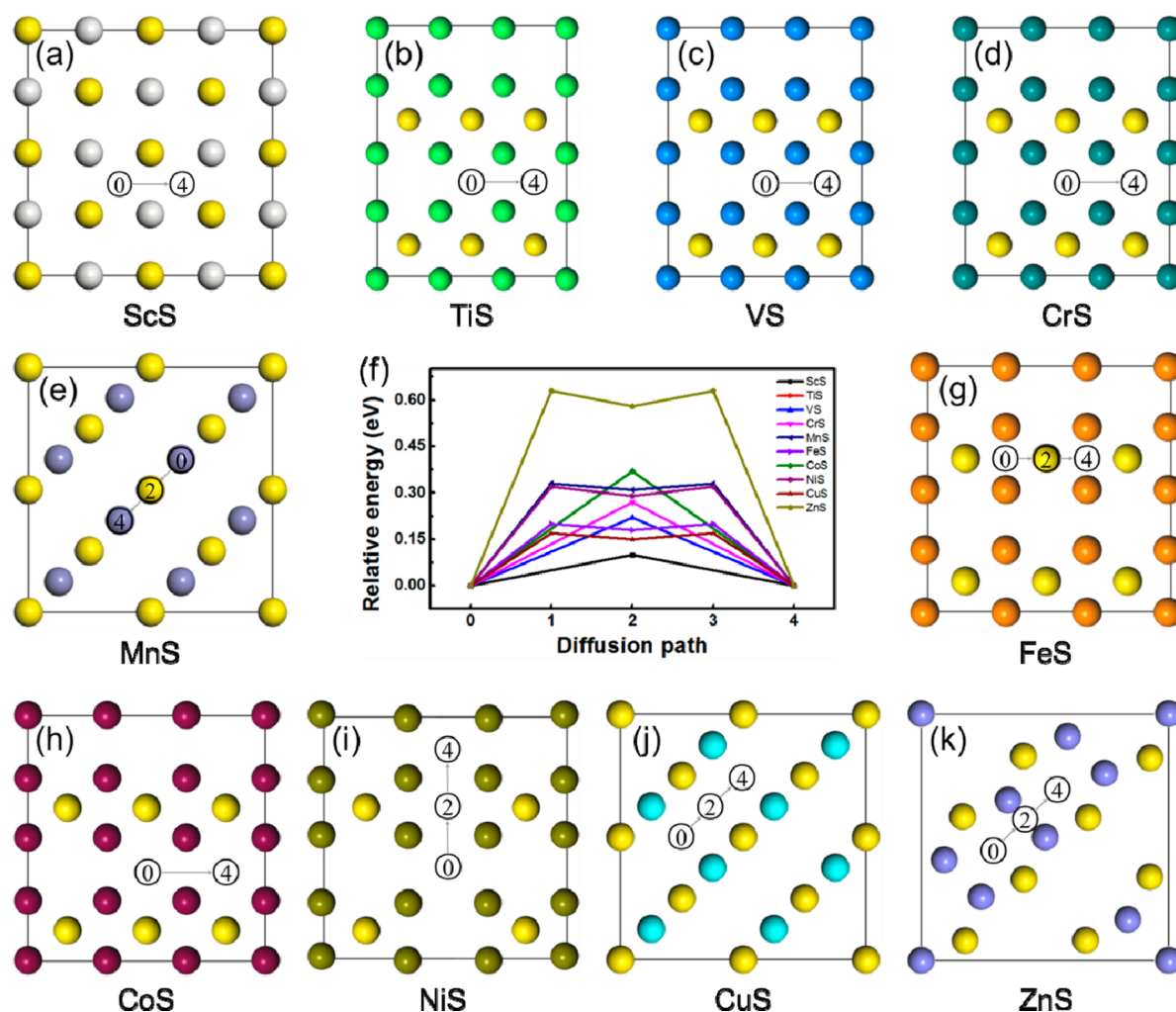


Figure 4. Lithium ion diffusion path on the surface of (a) ScS, (b) TiS, (c) VS, (d) CrS, (e) MnS, (g) FeS, (h) CoS, (i) NiS, (j) CuS, and (k) ZnS. (f) Energy profiles for diffusion processes of Li ion on first-row TMSs surface. The atomic colors are as same as that in Figure 2.

performance. Lithium ion diffusion barrier has been reported as a good descriptor to judge the surface properties of TMSs. A lower barrier can lead to an increase in the diffusion rate according to the exponential law. Then faster diffusion is beneficial to the intercalation–deintercalation of lithium and can promote the reaction between lithium and sulfur.<sup>42</sup> The corresponding results are summarized in Figures 4 and S6 and Table S5.

Generally, there are two kinds of diffusion pathways: unimodal curve (ScS, TiS, VS, CrS, and CoS), corresponding to one single transition-state point, and bimodal curve (MnS, FeS, NiS, CuS, and ZnS), in which a metastable point exists between two stable points. Half of the calculated TMSs have a lithium ion diffusion barrier lower than that of graphene materials, which is 0.31 eV (Figure S7). The lithium ion diffusion barrier on graphene is consistent with recent reports.<sup>58,59</sup> Among all the TMSs, VS has a small lithium ion diffusion barrier of 0.22 eV, and that of ScS is only 0.10 eV, which is the smallest. By comparison, ZnS has the largest lithium ion diffusion barrier of 0.63 eV. Based on the cyclic voltammetry (CV) measurements and the classical Randles–Sevcik equation, the higher Li-ion diffusion rate on VS<sub>2</sub> surface than graphene was confirmed experimentally, verifying our calculation results to some degree.<sup>42</sup> This finding further verifies that VS is a potentially desirable sulfur host for Li–S

batteries. The lower barrier can lead to a faster diffusion rate, allowing homogeneous deposition of Li<sub>2</sub>S.

In conclusion, we have systematically investigated the first-row TMSs as polar hosts for sulfur cathodes in Li–S batteries to reveal a general rationale for sulfur host design. A periodic law is drawn from the theoretical calculations based on DFT. It is predicted that VS has the strongest anchoring effects on Li<sub>2</sub>S immobilization and a relatively low lithium ion diffusion barrier, consistent with current reports. The strong S-binding is mainly induced by charge transfer between TM atoms in TMS slabs and S atoms in Li<sub>2</sub>S, different from Li-binding mainly induced by dipole–dipole interactions. In addition, the PDOS analysis further demonstrates the essential role of TM in rendering S-binding configuration with stronger anchoring. This finding provides a general and practical principle for rationally designing sulfur cathode materials and screening unexplored materials, which will propel the development of high-energy-density and long-life Li–S batteries.

## ■ ASSOCIATED CONTENT

### Supporting Information

The Supporting Information is available free of charge on the ACS Publications website at DOI: 10.1021/acsenenergylett.7b00164.

Computational details, band structure, optimized structure, Mulliken charge, and bond analysis; the periodic law of binding energy; PDOS analyses; and transition-state search of lithium diffusion (PDF)

## AUTHOR INFORMATION

### Corresponding Author

\*E-mail: zhang-qiang@mails.tsinghua.edu.cn.

### ORCID

Bo Li: 0000-0001-8895-2054

Qiang Zhang: 0000-0002-3929-1541

### Author Contributions

<sup>†</sup>X.C. and H.-J.P. contributed equally to this work.

### Notes

The authors declare no competing financial interest.

## ACKNOWLEDGMENTS

This work was supported by National Key Research and Development Program (Nos. 2016YFA0202500 and 2015CB932500), National Natural Science Foundation of China (Nos. 21422604 and 21276141), and Tsinghua National Laboratory for Information Science and Technology. We thank Chen-Zi Zhao, Ze-Wen Zhang, Ge Zhang, and Ying-Zhi Sun for helpful discussions.

## REFERENCES

- (1) Bruce, P. G.; Freunberger, S. A.; Hardwick, L. J.; Tarascon, J. M. Li-O<sub>2</sub> and Li-S Batteries with High Energy Storage. *Nat. Mater.* **2012**, *11*, 19–29.
- (2) Manthiram, A.; Fu, Y.; Chung, S. H.; Zu, C.; Su, Y. S. Rechargeable Lithium-Sulfur Batteries. *Chem. Rev.* **2014**, *114*, 11751–11787.
- (3) Ogoke, O.; Wu, G.; Wang, X.; Casimir, A.; Ma, L.; Wu, T.; Lu, J. Effective Strategies for Stabilizing Sulfur for Advanced Lithium–Sulfur Batteries. *J. Mater. Chem. A* **2017**, *5*, 448–469.
- (4) Kang, W.; Deng, N.; Ju, J.; Li, Q.; Wu, D.; Ma, X.; Li, L.; Naebe, M.; Cheng, B. A Review of Recent Developments in Rechargeable Lithium-Sulfur Batteries. *Nanoscale* **2016**, *8*, 16541–16588.
- (5) Liu, M.; Qin, X.; He, Y.-B.; Li, B.; Kang, F. Recent Innovative Configurations in High-Energy Lithium–Sulfur Batteries. *J. Mater. Chem. A* **2017**, DOI: 10.1039/C7TA00290D.
- (6) Liang, J.; Sun, Z.-H.; Li, F.; Cheng, H.-M. Carbon Materials for Li–S Batteries: Functional Evolution and Performance Improvement. *Energy Storage Mater.* **2016**, *2*, 76–106.
- (7) Pang, Q.; Liang, X.; Kwok, C. Y.; Nazar, L. F. Review—the Importance of Chemical Interactions between Sulfur Host Materials and Lithium Polysulfides for Advanced Lithium-Sulfur Batteries. *J. Electrochem. Soc.* **2015**, *162*, A2567–A2576.
- (8) Seh, Z. W.; Sun, Y.; Zhang, Q.; Cui, Y. Designing High-Energy Lithium-Sulfur Batteries. *Chem. Soc. Rev.* **2016**, *45*, 5605–5634.
- (9) Liu, M.; Ye, F.; Li, W.; Li, H.; Zhang, Y. Chemical Routes toward Long-Lasting Lithium/Sulfur Cells. *Nano Res.* **2016**, *9*, 94–116.
- (10) Borchardt, L.; Oschatz, M.; Kaskel, S. Carbon Materials for Lithium Sulfur Batteries—Ten Critical Questions. *Chem. - Eur. J.* **2016**, *22*, 7324–7351.
- (11) Manthiram, A.; Chung, S. H.; Zu, C. Lithium-Sulfur Batteries: Progress and Prospects. *Adv. Mater.* **2015**, *27*, 1980–2006.
- (12) Peng, H. J.; Zhang, Z. W.; Huang, J. Q.; Zhang, G.; Xie, J.; Xu, W. T.; Shi, J. L.; Chen, X.; Cheng, X. B.; Zhang, Q. A Cooperative Interface for Highly Efficient Lithium-Sulfur Batteries. *Adv. Mater.* **2016**, *28*, 9551–9558.
- (13) Zhang, S. S. Liquid Electrolyte Lithium/Sulfur Battery: Fundamental Chemistry, Problems, and Solutions. *J. Power Sources* **2013**, *231*, 153–162.
- (14) Yin, Y. X.; Xin, S.; Guo, Y. G.; Wan, L. J. Lithium-Sulfur Batteries: Electrochemistry, Materials, and Prospects. *Angew. Chem., Int. Ed.* **2013**, *52*, 13186–13200.
- (15) Liu, X.; Huang, J. Q.; Zhang, Q.; Mai, L. Nanostructured Metal Oxides and Sulfides for Lithium-Sulfur Batteries. *Adv. Mater.* **2017**, *29*, 1601759.
- (16) Huang, J.-Q.; Zhang, Q.; Wei, F. Multi-Functional Separator/Interlayer System for High-Stable Lithium-Sulfur Batteries: Progress and Prospects. *Energy Storage Mater.* **2015**, *1*, 127–145.
- (17) Peng, H.-J.; Cheng, X.; Huang, J.; Zhang, Q. Review on High-Loading and High-Energy Lithium-Sulfur Batteries. *Adv. Energy Mater.* **2017**, *7*, 1700260.
- (18) Zhao, C.-Z.; Cheng, X.-B.; Zhang, R.; Peng, H.-J.; Huang, J.-Q.; Ran, R.; Huang, Z.-H.; Wei, F.; Zhang, Q. Li<sub>2</sub>S<sub>5</sub>-Based Ternary-Salt Electrolyte for Robust Lithium Metal Anode. *Energy Storage Mater.* **2016**, *3*, 77–84.
- (19) Chen, X.; Hou, T.-Z.; Li, B.; Yan, C.; Zhu, L.; Guan, C.; Cheng, X.-B.; Peng, H.-J.; Huang, J.-Q.; Zhang, Q. Towards Stable Lithium-Sulfur Batteries: Mechanistic Insights into Electrolyte Decomposition on Lithium Metal Anode. *Energy Storage Mater.* **2017**, DOI: 10.1016/j.ensm.2017.01.003.
- (20) Ji, X.; Lee, K. T.; Nazar, L. F. A Highly Ordered Nanostructured Carbon-Sulphur Cathode for Lithium-Sulphur Batteries. *Nat. Mater.* **2009**, *8*, 500–506.
- (21) Zhou, G.; Zhao, Y.; Manthiram, A. Dual-Confined Flexible Sulfur Cathodes Encapsulated in Nitrogen-Doped Double-Shelled Hollow Carbon Spheres and Wrapped with Graphene for Li-S Batteries. *Adv. Energy Mater.* **2015**, *5*, 1402263.
- (22) Cheng, X.-B.; Huang, J.-Q.; Zhang, Q.; Peng, H.-J.; Zhao, M.-Q.; Wei, F. Aligned Carbon Nanotube/Sulfur Composite Cathodes with High Sulfur Content for Lithium–Sulfur Batteries. *Nano Energy* **2014**, *4*, 65–72.
- (23) Fei, L.; Li, X.; Bi, W.; Zhuo, Z.; Wei, W.; Sun, L.; Lu, W.; Wu, X.; Xie, K.; Wu, C.; et al. Graphene/Sulfur Hybrid Nanosheets from a Space-Confined “Sauna” Reaction for High-Performance Lithium-Sulfur Batteries. *Adv. Mater.* **2015**, *27*, 5936–5942.
- (24) Wang, Z.; Dong, Y.; Li, H.; Zhao, Z.; Wu, H. B.; Hao, C.; Liu, S.; Qiu, J.; Lou, X. W. Enhancing Lithium-Sulphur Battery Performance by Strongly Binding the Discharge Products on Amino-Functionalized Reduced Graphene Oxide. *Nat. Commun.* **2014**, *5*, 5002.
- (25) Zhou, G.; Paek, E.; Hwang, G. S.; Manthiram, A. Long-Life Li/Polysulphide Batteries with High Sulphur Loading Enabled by Lightweight Three-Dimensional Nitrogen/Sulphur-Codoped Graphene Sponge. *Nat. Commun.* **2015**, *6*, 7760.
- (26) Zhou, G.; Yin, L.-C.; Wang, D.-W.; Li, L.; Pei, S.; Gentle, I. R.; Li, F.; Cheng, H.-M. Fibrous Hybrid of Graphene and Sulfur Nanocrystals for High-Performance Lithium–Sulfur Batteries. *ACS Nano* **2013**, *7*, 5367–5375.
- (27) Tang, C.; Li, B.-Q.; Zhang, Q.; Zhu, L.; Wang, H.-F.; Shi, J.-L.; Wei, F. Cao-Templated Growth of Hierarchical Porous Graphene for High-Power Lithium-Sulfur Battery Applications. *Adv. Funct. Mater.* **2016**, *26*, 577–585.
- (28) Ji, L.; Rao, M.; Zheng, H.; Zhang, L.; Li, Y.; Duan, W.; Guo, J.; Cairns, E. J.; Zhang, Y. Graphene Oxide as a Sulfur Immobilizer in High Performance Lithium/Sulfur Cells. *J. Am. Chem. Soc.* **2011**, *133*, 18522–18525.
- (29) Seh, Z. W.; Wang, H.; Liu, N.; Zheng, G.; Li, W.; Yao, H.; Cui, Y. High-Capacity Li<sub>2</sub>S–Graphene Oxide Composite Cathodes with Stable Cycling Performance. *Chem. Sci.* **2014**, *5*, 1396–1400.
- (30) Zhao, M. Q.; Liu, X. F.; Zhang, Q.; Tian, G. L.; Huang, J. Q.; Zhu, W.; Wei, F. Graphene/Single-Walled Carbon Nanotube Hybrids: One-Step Catalytic Growth and Applications for High-Rate Li-S Batteries. *ACS Nano* **2012**, *6*, 10759–10769.
- (31) Peng, H.-J.; Huang, J.-Q.; Zhao, M.-Q.; Zhang, Q.; Cheng, X.-B.; Liu, X.-Y.; Qian, W.-Z.; Wei, F. Nanoarchitected Graphene/CNT@Porous Carbon with Extraordinary Electrical Conductivity and Interconnected Micro/Mesopores for Lithium-Sulfur Batteries. *Adv. Funct. Mater.* **2014**, *24*, 2772–2781.

- (32) Song, J.; Gordin, M. L.; Xu, T.; Chen, S.; Yu, Z.; Sohn, H.; Lu, J.; Ren, Y.; Duan, Y.; Wang, D. Strong Lithium Polysulfide Chemisorption on Electroactive Sites of Nitrogen-Doped Carbon Composites for High-Performance Lithium-Sulfur Battery Cathodes. *Angew. Chem., Int. Ed.* **2015**, *54*, 4325–4329.
- (33) Ding, Y.-L.; Kopold, P.; Hahn, K.; van Aken, P. A.; Maier, J.; Yu, Y. Facile Solid-State Growth of 3D Well-Interconnected Nitrogen-Rich Carbon Nanotube-Graphene Hybrid Architectures for Lithium-Sulfur Batteries. *Adv. Funct. Mater.* **2016**, *26*, 1112–1119.
- (34) Yin, L.-C.; Liang, J.; Zhou, G.-M.; Li, F.; Saito, R.; Cheng, H.-M. Understanding the Interactions between Lithium Polysulfides and N-Doped Graphene Using Density Functional Theory Calculations. *Nano Energy* **2016**, *25*, 203–210.
- (35) Hou, T. Z.; Peng, H. J.; Huang, J. Q.; Zhang, Q.; Li, B. The Formation of Strong-Couple Interactions between Nitrogen-Doped Graphene and Sulfur/Lithium (Poly)Sulfides in Lithium-Sulfur Batteries. *2D Mater.* **2015**, *2*, 014011.
- (36) Peng, H.-J.; Hou, T.-Z.; Zhang, Q.; Huang, J.-Q.; Cheng, X.-B.; Guo, M.-Q.; Yuan, Z.; He, L.-Y.; Wei, F. Strongly Coupled Interfaces between a Heterogeneous Carbon Host and a Sulfur-Containing Guest for Highly Stable Lithium-Sulfur Batteries: Mechanistic Insight into Capacity Degradation. *Adv. Mater. Interfaces* **2014**, *1*, 1400227.
- (37) Hou, T. Z.; Chen, X.; Peng, H. J.; Huang, J. Q.; Li, B. Q.; Zhang, Q.; Li, B. Design Principles for Heteroatom-Doped Nanocarbon to Achieve Strong Anchoring of Polysulfides for Lithium-Sulfur Batteries. *Small* **2016**, *12*, 3283–3291.
- (38) Xu, N.; Qian, T.; Liu, X.; Liu, J.; Chen, Y.; Yan, C. Greatly Suppressed Shuttle Effect for Improved Lithium Sulfur Battery Performance through Short Chain Intermediates. *Nano Lett.* **2017**, *17*, 538–543.
- (39) Yuan, S.; Bao, J. L.; Wang, L.; Xia, Y.; Truhlar, D. G.; Wang, Y. Graphene-Supported Nitrogen and Boron Rich Carbon Layer for Improved Performance of Lithium-Sulfur Batteries Due to Enhanced Chemisorption of Lithium Polysulfides. *Adv. Energy Mater.* **2016**, *6*, 1501733.
- (40) Jin, C.; Zhang, W.; Zhuang, Z.; Wang, J.; Huang, H.; Gan, Y.; Xia, Y.; Liang, C.; Zhang, J.; Tao, X. Enhanced Sulfide Chemisorption Using Boron and Oxygen Dually Doped Multi-Walled Carbon Nanotubes for Advanced Lithium–Sulfur Batteries. *J. Mater. Chem. A* **2017**, *5*, 632–640.
- (41) Peng, H. J.; Zhang, G.; Chen, X.; Zhang, Z. W.; Xu, W. T.; Huang, J. Q.; Zhang, Q. Enhanced Electrochemical Kinetics on Conductive Polar Mediators for Lithium-Sulfur Batteries. *Angew. Chem., Int. Ed.* **2016**, *55*, 12990–12995.
- (42) Zhou, G.; Tian, H.; Jin, Y.; Tao, X.; Liu, B.; Zhang, R.; Seh, Z. W.; Zhuo, D.; Liu, Y.; Sun, J.; et al. Catalytic Oxidation of  $\text{Li}_2\text{S}$  on the Surface of Metal Sulfides for Li-S Batteries. *Proc. Natl. Acad. Sci. U. S. A.* **2017**, *114*, 840–845.
- (43) Zhang, Q.; Wang, Y.; Seh, Z. W.; Fu, Z.; Zhang, R.; Cui, Y. Understanding the Anchoring Effect of Two-Dimensional Layered Materials for Lithium-Sulfur Batteries. *Nano Lett.* **2015**, *15*, 3780–3786.
- (44) Cui, Z.; Zu, C.; Zhou, W.; Manthiram, A.; Goodenough, J. B. Mesoporous Titanium Nitride-Enabled Highly Stable Lithium-Sulfur Batteries. *Adv. Mater.* **2016**, *28*, 6926–6931.
- (45) Liang, X.; Garsuch, A.; Nazar, L. F. Sulfur Cathodes Based on Conductive Mxene Nanosheets for High-Performance Lithium-Sulfur Batteries. *Angew. Chem., Int. Ed.* **2015**, *54*, 3907–3911.
- (46) Bao, W.; Su, D.; Zhang, W.; Guo, X.; Wang, G. 3D Metal Carbide@Mesoporous Carbon Hybrid Architecture as a New Polysulfide Reservoir for Lithium-Sulfur Batteries. *Adv. Funct. Mater.* **2016**, *26*, 8746–8756.
- (47) Wang, X.; Gao, T.; Fan, X.; Han, F.; Wu, Y.; Zhang, Z.; Li, J.; Wang, C. Tailoring Surface Acidity of Metal Oxide for Better Polysulfide Entrapment in Li-S Batteries. *Adv. Funct. Mater.* **2016**, *26*, 7164–7169.
- (48) Zhao, T.; Ye, Y.; Peng, X.; Divitini, G.; Kim, H.-K.; Lao, C.-Y.; Coxon, P. R.; Xi, K.; Liu, Y.; Ducati, C.; et al. Advanced Lithium-Sulfur Batteries Enabled by a Bio-Inspired Polysulfide Adsorptive Brush. *Adv. Funct. Mater.* **2016**, *26*, 8418–8426.
- (49) Tao, X.; Wang, J.; Ying, Z.; Cai, Q.; Zheng, G.; Gan, Y.; Huang, H.; Xia, Y.; Liang, C.; Zhang, W.; et al. Strong Sulfur Binding with Conducting Magneli-Phase  $\text{Ti}_n\text{O}_{2n-1}$  Nanomaterials for Improving Lithium-Sulfur Batteries. *Nano Lett.* **2014**, *14*, 5288–5294.
- (50) Tao, X.; Wang, J.; Liu, C.; Wang, H.; Yao, H.; Zheng, G.; Seh, Z. W.; Cai, Q.; Li, W.; Zhou, G.; et al. Balancing Surface Adsorption and Diffusion of Lithium-Polysulfides on Nonconductive Oxides for Lithium-Sulfur Battery Design. *Nat. Commun.* **2016**, *7*, 11203.
- (51) Pang, Q.; Kundu, D.; Nazar, L. F. A Graphene-Like Metallic Cathode Host for Long-Life and High-Loading Lithium–Sulfur Batteries. *Mater. Horiz.* **2016**, *3*, 130–136.
- (52) Yuan, Z.; Peng, H. J.; Hou, T. Z.; Huang, J. Q.; Chen, C. M.; Wang, D. W.; Cheng, X. B.; Wei, F.; Zhang, Q. Powering Lithium-Sulfur Battery Performance by Propelling Polysulfide Redox at Sulfiphilic Hosts. *Nano Lett.* **2016**, *16*, 519–527.
- (53) Seh, Z. W.; Yu, J. H.; Li, W.; Hsu, P. C.; Wang, H.; Sun, Y.; Yao, H.; Zhang, Q.; Cui, Y. Two-Dimensional Layered Transition Metal Disulfides for Effective Encapsulation of High-Capacity Lithium Sulfide Cathodes. *Nat. Commun.* **2014**, *5*, 5017.
- (54) Jain, A.; Ong, S. P.; Hautier, G.; Chen, W.; Richards, W. D.; Dacek, S.; Cholia, S.; Gunter, D.; Skinner, D.; Ceder, G.; et al. Commentary: The Materials Project: A Materials Genome Approach to Accelerating Materials Innovation. *APL Mater.* **2013**, *1*, 011002.
- (55) Hammer, B.; Nørskov, J. K. Electronic Factors Determining the Reactivity of Metal Surfaces. *Surf. Sci.* **1995**, *343*, 211–220.
- (56) Greeley, J.; Nørskov, J. K.; Mavrikakis, M. Electronic Structure and Catalysis on Metal Surfaces. *Annu. Rev. Phys. Chem.* **2002**, *53*, 319–348.
- (57) Xin, H.; Linic, S. Communications: Exceptions to the  $d$ -Band Model of Chemisorption on Metal Surfaces: The Dominant Role of Repulsion between Adsorbate States and Metal  $d$ -States. *J. Chem. Phys.* **2010**, *132*, 221101.
- (58) Zhou, L.-J.; Hou, Z. F.; Wu, L.-M. First-Principles Study of Lithium Adsorption and Diffusion on Graphene with Point Defects. *J. Phys. Chem. C* **2012**, *116*, 21780–21787.
- (59) Uthaisar, C.; Barone, V. Edge Effects on the Characteristics of Li Diffusion in Graphene. *Nano Lett.* **2010**, *10*, 2838–2842.